



Characterizing caspase-1 involvement during esophageal disease progression

Gillian Barber^{1,2} · Akanksha Anand³ · Katarzyna Oficjalska¹ · James J. Phelan² · Aisling B. Heeran² · Ewelina Flis¹ · Niamh E. Clarke² · Jenny A. Watson⁴ · Julia Strangmann³ · Brian Flood¹ · Hazel O'Neill² · Dermot O'Toole⁵ · Finbar MacCarthy⁵ · Narayanasamy Ravi^{2,5} · John V. Reynolds^{2,5} · Elaine W. Kay⁴ · Michael Quante³ · Jacintha O'Sullivan² · Emma M. Creagh¹

Received: 20 February 2020 / Accepted: 19 June 2020 / Published online: 1 July 2020
© Springer-Verlag GmbH Germany, part of Springer Nature 2020

Abstract

Barrett's esophagus (BE) is an inflammatory condition and a neoplastic precursor to esophageal adenocarcinoma (EAC). Inflammasome signaling, which contributes to acute and chronic inflammation, results in caspase-1 activation leading to the secretion of IL-1 β and IL-18, and inflammatory cell death (pyroptosis). This study aimed to characterize caspase-1 expression, and its functional importance, during disease progression to BE and EAC. Three models of disease progression (Normal–BE–EAC) were employed to profile caspase-1 expression: (1) a human esophageal cell line model; (2) a murine model of BE; and (3) resected tissue from BE-associated EAC patients. BE patient biopsies and murine BE organoids were cultured *ex vivo* in the presence of a caspase-1 inhibitor, to determine the importance of caspase-1 for inflammatory cytokine and chemokine secretion.

Epithelial caspase-1 expression levels were significantly enhanced in BE ($p < 0.01$). In contrast, stromal caspase-1 levels correlated with histological inflammation scores during disease progression ($p < 0.05$). Elevated secretion of IL-1 β from BE explanted tissue, compared to adjacent normal tissue ($p < 0.01$), confirmed enhanced activity of caspase-1 in BE tissue. Caspase-1 inhibition in LPS-stimulated murine BE organoids caused a significant reduction in IL-1 β ($p < 0.01$) and CXCL1 ($p < 0.05$) secretion, confirming the importance of caspase-1 in the production of cytokines and chemokines associated with disease progression from BE to EAC. Targeting caspase-1 activity in BE patients should therefore be tested as a novel strategy to prevent inflammatory complications associated with disease progression.

Keywords Esophageal cancer · Inflammation · Barrett's metaplasia · Inflammasome

Abbreviations

CRC	Colitis-associated colorectal cancer
EAC	Esophageal adenocarcinoma
HGD	High-grade dysplasia
IFN- γ	Interferon-gamma
IHC	Immunohistochemistry
IL	Interleukin
LDH	Lactate dehydrogenase

LGD	Low-grade dysplasia
NLRP	Nod-like receptor protein
SCJ	Squamocolumnar junction
TNF α	Tumor necrosis factor alpha

Introduction

Barrett's esophagus (BE) is an inflammation-driven, pre-neoplastic condition that is part of a pathological sequence of events predisposing to esophageal adenocarcinoma (EAC) [1, 2]. BE is defined by the replacement of normal squamous epithelium with specialized intestinal metaplasia in the distal esophagus [3]. With disease progression, BE patients may develop features of low- and high-grade dysplasia leading to an increased risk of EAC. Nonetheless, annual risk of developing BE-associated EAC is relatively low at 0.12% [4]. BE

Electronic supplementary material The online version of this article (<https://doi.org/10.1007/s00262-020-02650-4>) contains supplementary material, which is available to authorized users.

✉ Jacintha O'Sullivan
osullij4@tcd.ie

✉ Emma M. Creagh
ecreagh@tcd.ie

Extended author information available on the last page of the article

patients currently undergo surveillance endoscopies, despite the low rates of progression [3]. As inflammation seems to be a main driver of tumor progression, a better understanding of inflammatory pathways during disease progression is required to improve preventive strategies [5].

Caspase-1 is a member of the inflammatory caspase subfamily, which also includes caspase-4 and -5 in humans and caspase-11 in mice [6]. Once activated, caspase-1 is responsible for the direct cleavage and subsequent secretion of the potent inflammatory cytokines IL-1 β and IL-18 as part of the canonical inflammasome pathway [7]. The activation of caspase-1 also results in an inflammatory form of cell death, termed pyroptosis, which requires gasdermin D (GSDMD) cleavage [8]. Importantly, caspase-1 activation is an outcome of all inflammasome pathways and is therefore a meaningful indicator for inflammasome-associated inflammation [9]. Caspase-4 and -5 have also been shown to regulate and activate the inflammasome through the non-canonical pathway [6].

BE is an inflammatory condition with elevated levels of chemokines and cytokines, including the neutrophil chemoattractant IL-8 and pro-inflammatory cytokine IL-1 β [10, 11]. The influence of inflammatory chemokine and cytokine levels on esophageal disease progression is supported by a recent study which identifies a correlation between increasing neutrophil–lymphocyte ratio (NLR) and neoplastic progression [12]. Furthermore, overexpression of mature IL-1 β in the esophagus of mice is responsible for the transgenic BE model, L2-IL-1B [13]. This model highlights the importance of inflammasome pathways in disease development. IL-1 β stimulates autocrine signaling to induce BE pathogenesis in the absence of additional risk factors such as bile acid exposure or obesity [13].

The inflammasome sensor proteins NLRP1, NLRP3 and AIM2 are expressed in normal esophageal tissue (www.proteinatlas.org) [14], which are potentially primed through stimuli present in the distal esophagus, leading to enhanced inflammation. This scenario has already been indicated for the NLRP3 inflammasome during BE [15].

We hypothesize that caspase-1-mediated inflammation has a role in the pathogenesis of BE and progression to EAC. We provide evidence that caspase-1 is highly expressed in BE and EAC. Ex vivo inhibition of caspase-1 in BE patient biopsies and in murine BE organoid cultures reduced inflammatory cytokine and chemokine secretion, suggesting that caspase-1 inhibition may represent a novel strategy to prevent inflammatory acceleration of esophageal carcinogenesis.

Materials and methods

Esophageal cell line model of disease

Cell lines Het-1A (normal squamous, RRID: CVCL_3702), QH (CP-A, metaplasia, RRID: CVCL_C451), GO

(CP-B, high-grade dysplasia, RRID: CVCL_C452), OE33 (EAC, RRID: CVCL_0471) and SKGT4 (EAC, RRID: CVCL_2195) represent stages of disease progression. All lines, except OE33 and SKGT4 (ECACC), were obtained from ATCC. Het-1A, QH and GO were cultured in BEGM™ Bronchial Epithelial Cell Growth Medium Bullet kit (Lonza). OE33, SKGT4 and THP-1 (RRID: CVCL_0006) cell lines were cultured in RPMI 1640 GlutaMAX™, 10% FBS (Labtech), and penicillin–streptomycin (100 U/mL, 100 μ g/mL).

Immunoblotting

20 μ g protein lysate was run on 12% SDS-PAGE gels, transferred to nitrocellulose, and probed with primary antibodies: anti-caspase-1 (1:500, RRID: AB_2069053); anti-caspase-4 (1:1000, RRID: AB_590743); anti-caspase-5 (1:1000, RRID: AB_590746); anti- β -actin (1:10,000, RRID: AB_262011); followed by HRP-secondary antibody (Jackson ImmunoLabs). Immunoblots were coated with enhanced chemiluminescent (ECL) substrate (Millipore) and developed using the BioRad ChemiDoc™ MP Imaging System. Densitometric analysis was performed using Biorad Image Lab software.

Animal studies

The L2-IL-1B mice used were developed by backcrossing C57BL/6J mice with the mouse model (L2-IL1B, Tg[ED-L2-IL1RN/IL1B]#tcw), which involved targeting IL-1 β expression to the squamous epithelium of the mouse using an Epstein Barr virus L2 promoter [13, 16]. Mice included both genders, were monitored daily and were fed a standard chow diet and water ad libitum.

For histology, mice of four different age groups (3, 6, 9 and 12 months) representing disease progression were killed by isoflurane overdose ($n = 5$ per group). The esophagus and stomach of L2-IL-1B mice were resected, formalin fixed (10%) and paraffin embedded. Histological scoring was performed by an experienced mouse pathologist using a blinded scoring system (Supplementary Table I) [5]. This system used previously established criteria for the influx of immune cells per high-power field, metaplasia, and neoplastic progression in mice [5, 13, 17]. Inflammation represents a score of all immune cells within a defined area of tissue around the squamocolumnar junction (SCJ), predominantly made up of neutrophil myeloid cells. Metaplasia was assessed through identification of mucus producing cells per gland, and the number of glands with mucus producing cells in the BE area. Neoplastic progression was evaluated using the following scoring criteria:

0—no neoplastic progression; 1—‘superficial epithelial atypia’ describes a phenotype that includes more than just mucus cell metaplasia, with single cells showing nuclear enlargement in selected crypts within the BE area at the squamous–columnar junction; 2—‘atypia in granular complexity’ describes a phenotype that includes more than just mucus cell metaplasia, with multiple spanning cells showing nuclear enlargement and stratification in multiple crypts within the BE area at the squamous–columnar junction; 3—‘low-grade dysplasia’ describes a phenotype that has some alterations in crypt structure, with cells showing hyperchromatic nuclei with mild crowding and stratification; 4—‘high-grade dysplasia’ describes a phenotype which has a distorted crypt architecture with size irregularity, budding and crowding (back-to-back) crypts, loss of nuclear polarity, markedly enlarged, overlapping and hyperchromatic nuclei with dysplastic epithelium on mucosal surface. Goblet cell ratio was assessed by determining whether each crypt consisting of columnar epithelium was positive or negative for goblet cells. The number of positive crypts was then divided by the total number of crypts and defined as a percentage (%) [5, 18].

Immunohistochemistry (IHC) was performed using the Vectastain ABC DAB detection kit (Vector Labs) for each mice age group. Sections were deparaffinized, rehydrated and heated; antigen retrieval was carried out in 10 mM citrate buffer (pH 6.0, 15 min). Tissue was blocked (3% BSA, 5% goat serum) and quenched (3% H₂O₂) prior to incubation with anti-caspase-1 (1:50, RRID: AB_1660708), followed by secondary antibody (Vector Labs). Appropriate negative controls (primary antibody omitted) were used. Imaging was performed using Aperio ImageScope viewing software (Leica Biosystems). Scoring was performed by two blinded reviewers (G.B., A.A./E.F.) using a validated semi-quantitative scoring system [5]. Caspase-1 expression was assessed in the epithelium and stroma for percent positivity within the BE region.

Murine BE organoid culture

For organoid culture, cells were taken from the cardia region at the SCJ of 12-month-old L2-IL-1B mice and cultured as 3D organoids in Matrigel for 3 weeks, as previously described [19]. Three days prior to harvesting, organoids were pre-treated (1 h) with caspase-1 inhibitor, WEHD.CHO (50 μ M) before 24-h stimulation with LPS (1 μ g/mL). The following day, media were replaced and re-treated with inhibitor and LPS for a further 24 h. Organoid diameters (μ m) were assessed under a light microscope (Zeiss, Axiovert 200 M) and analyzed (ImageJ software, Fiji) at 0 h (before treatment), 24 h (during treatment) and 48 h (before harvest).

BE-associated EAC patient tissue

All patients, recruited in the Irish national referral center for upper GI malignancy, were histologically confirmed with BE-associated EAC. Formalin-fixed, paraffin-embedded esophagectomy tissue was retrieved from 32 EAC patients. Defined areas of tumor, islands of BE and adjacent normal mucosa were identified by an experienced histopathologist (E.K.). Tissue microarrays (TMAs) were constructed by taking three tissue cores from each histologically defined tissue area, 4 μ m sections were placed on glass slides and heated overnight (37 °C).

IHC staining was performed using the Leica Bond-III fully automated tissue stainer (Leica Biosystems). Slides were dewaxed before pre-treatment with Bond Epitope Retrieval Solution I. Primary antibody, anti-caspase-1 (1:250 dilution, RRID: AB_2069053), was diluted in Bond Primary Antibody Diluent. Detection and visualization of stained cells was achieved using the Bond Polymer Refine Detection Kit, using DAB chromogen. Caspase-1 expression was assessed by two blinded reviewers (K.O., J.P.) using a validated semi-quantitative scoring method [20].

Optimization of caspase-1 inhibitor dose in THP-1 cells

Dose response [1, 5, 10 μ M] of caspase-1 inhibitor, WEHD.CHO (Trp-Glu-His-Asp-aldehyde, Calbiochem) was carried in the THP-1 cell line (ATCC). WEHD.CHO was chosen for its reported superior caspase-1 specificity [21–23]. THP-1 cells were differentiated to macrophages (10 ng/mL PMA, 48 h), before priming overnight with LPS (1 μ g/mL, Sigma). NLRP3 inflammasome activation was induced using ATP (5 mM, 30 min). Caspase-1 activity was determined by quantifying IL-1 β secretion in supernatants.

Ex vivo BE patient explant culture

Histologically confirmed patients with BE were prospectively recruited from St. James’s Hospital. BE biopsies were taken from identified areas of metaplasia, while matched adjacent squamous tissue was taken \geq 5 cm from the proximal border of the BE region. Two matched biopsies were used per treatment group (4 metaplasia, 4 normal adjacent per patient). Ex vivo matched normal and metaplastic biopsies were cultured in conditioned M199 media and treated with or without caspase-1 inhibitor (10 μ M WEHD.CHO dissolved in H₂O, 16 h) before supernatant collection. Inhibitor cytotoxicity was tested by measuring LDH secretion (CytoTox96[®], Promega).

Quantification of cytokine secretion

Cytokine levels in supernatants from ex vivo biopsy and murine organoid incubations were quantified by ELISA. For mouse work: IL-1 β and IL-6 were used (MesoScale Diagnostics multiplex) and CXCL1 and CXCL2 (R&D Systems). For human work: IL-1 β , IL-6 and TNF α (MesoScale Diagnostics multiplex); IL-8, IL-1 α , IFN- γ (BioLegend®); IL-18 (R&D Systems) were used. All assays were performed as per manufacturer's protocols. Cytokine levels were normalized to total protein content per biopsy/organoid culture (pg/ μ g).

Statistical analysis

GraphPad Prism 5 software was used for statistical analysis, represented as mean \pm SEM. Cell line and mouse experiments were analyzed using one-way ANOVA, followed by Tukey's post hoc test. Clinical data were analyzed using Wilcoxon signed-rank test, one-way ANOVA followed by Tukey's post hoc test or two-way ANOVA followed by Bonferroni's post-test. Correlation analysis was performed using Spearman's correlation coefficient. Statistical significance $p < 0.05$.

Results

A cell line model of BE to EAC progression reveals strong expression of caspase-1

To determine inflammatory caspase expression during disease progression to EAC, an esophageal cell line model representing different stages of disease was employed. The cell lines used were: normal squamous (Het-1A), BE (QH), high-grade dysplasia (GO), well-differentiated EAC (SKGT4), and poorly differentiated EAC (OE33) (Fig. 1a). LPS-stimulated THP-1 cells served as positive control. Expression of the inflammatory caspases-1, -4 and -5 in each cell line was assessed, as all three caspases are capable of regulating inflammasome pathway activities [6]. Immunoblots and densitometry graphs represent relative protein expression of the inflammatory caspases (Fig. 1b, c). Caspase-1 was highly expressed in the metaplastic cell line ($p < 0.01$), while two EAC cell lines ($p < 0.01$) had undetectable levels of caspase-1. Caspase-4 expression was increased in the OAC cell line, OE33, although not significantly. In contrast, no significant differences in caspase-5 expression were detected across the cell lines.

Characterization of disease progression in the L2-IL-1B mouse model of BE

Observations from the cell line model of progression suggested that caspase-1 may be upregulated during

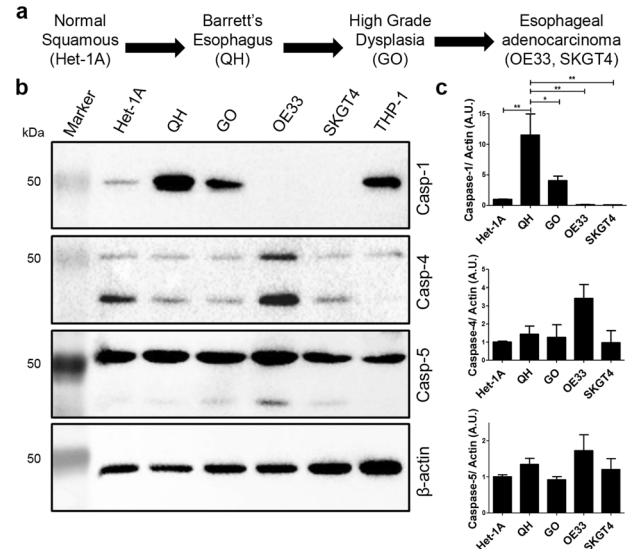


Fig. 1 A cell line model of EAC progression reveals strong expression of caspase-1. **a** Cell lines representative of EAC progression: Het-1A (normal squamous), QH (BE), GO (high-grade dysplasia), OE33 and SKGT4 (EAC) and THP-1 (positive control). **b** Western blot analysis and **c** subsequent densitometric analysis (arbitrary units) of inflammatory caspase-1 (45 kDa), caspase-4 (43.2 kDa, 36.7 kDa) and caspase-5 (49.7 kDa, 33.3 kDa) in esophageal cell lines. 20 μ g lysate was loaded/well of a 12% SDS-PAGE gel (Biorad). Immunoblots are representative of three independent experiments. Densitometry data represents mean \pm SEM ($n = 3$), normalized to loading control, β -actin using Biorad Image Lab software. One-way ANOVA followed by Tukey's post hoc test: * $p < 0.05$, ** $p < 0.01$

metaplasia. We next sought to identify caspase-1 expression levels during disease development stages in the L2-IL-1B transgenic mouse model of BE [13].

We characterized disease development over time in L2-IL-1B mice using H&E staining. Figure 2a shows representative images of the BE region in groups of mice aged 3, 6, 9 and 12 months. Histological analysis revealed development of inflammation and early evidence of metaplasia at 3 months (Fig. 2b, c), with established metaplasia ($p < 0.001$) within 6 months (Fig. 2c). At 9 months, histological scores reveal well-established inflammation ($p < 0.05$) and metaplasia ($p < 0.001$), with characteristics of early murine neoplasia ($p < 0.05$) (Fig. 2a-e). 12-month-old mice reveal the most progressed disease phenotype, distinguished by features of early neoplasia ($p < 0.01$), and reduced goblet cell ratio ($p < 0.05$). Goblet cells are proposed to be protective in BE, while reductions in goblet cell ratios may indicate increased susceptibility to neoplasia [18]. Collectively, the histological scores confirm that L2-IL-1B mice develop metaplasia within 6 months and advance to early murine neoplastic tissue formations at the SCJ in the following months [13].

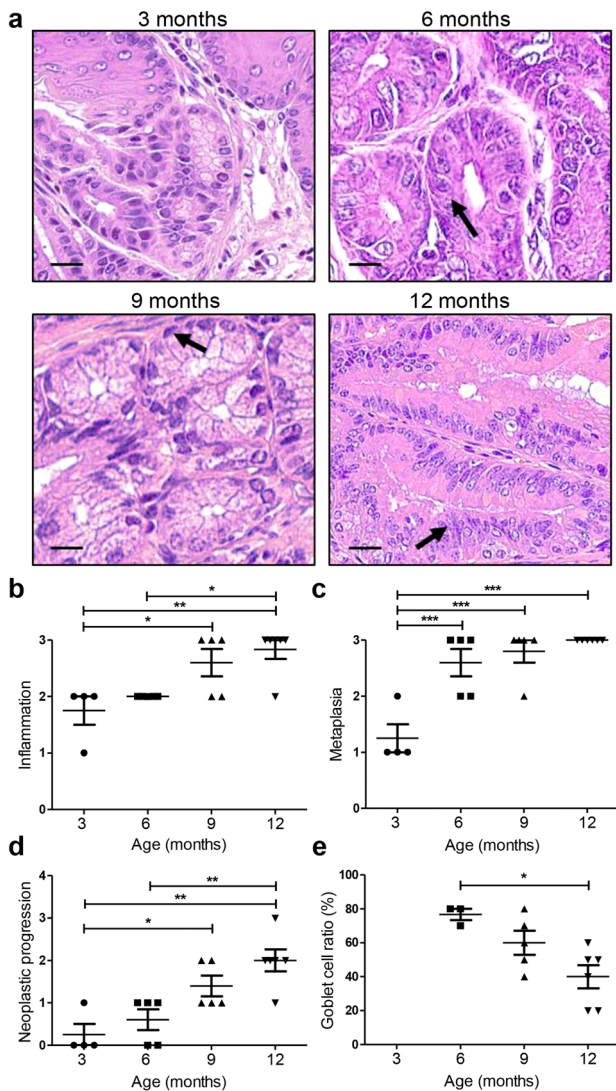


Fig. 2 Characterization of disease progression in the L2-IL-1B mouse model of BE. **a** Representative H and E stained images of the BE region at the SCJ in L2-IL-1B mice at 3 ($n=4$), 6 ($n=5$), 9 ($n=5$) and 12 ($n=5$) months (Aperio ImageScope, Leica). Arrows: 1) columnar epithelium, 2) well-differentiated goblet-like cells, 3) nuclear misalignment and crowding in early neoplastic columnar cells. Magnification $20\times$, scale bars= $20\mu\text{m}$. **b** Histological scores for inflammation (scale: 0=no inflammation, 1=mild, 2=moderate, 3=severe). **c** Histological scores for metaplasia (scale: 0=no metaplasia, 1=rare mucous cells, 2=single metaplastic glands, 3= multiple metaplastic glands). **d** Histological scores for neoplastic progression (scale: 0=no neoplastic progression, 1=superficial epithelial atypia, 2=atypia with granular complexity, 3=low-grade dysplasia, 4=high-grade dysplasia). **e** Goblet cell ratio (%) calculated as a percentage of goblet cell positivity within each crypt in the BE region. Data represent mean \pm SEM. One-way ANOVA, followed by Tukey's post hoc test: * $p < 0.05$, ** $p < 0.01$, *** $p < 0.001$

Epithelial caspase-1 expression is upregulated during BE metaplasia in L2-IL-1B mice.

To determine caspase-1 expression levels during the establishment of metaplasia, tissue sections from the SCJ of L2-IL-1B mice were IHC stained and scored for caspase-1 expression within the metaplastic regions [5]. Wild-type mice were excluded as no intestinal metaplasia was present in these mice, and therefore received a score of zero. Epithelial caspase-1 levels were substantially upregulated ($p < 0.001$) in 9-month-old mice at the SCJ when metaplasia was fully established (Fig. 3a, b). Observations from the L2-IL-1B BE model are therefore in agreement with data generated from the cell line model of disease development, where the metaplastic cell line had significant levels of caspase-1, while tumor cell lines had poor expression (Fig. 1c). This further supports our hypothesis that epithelial caspase-1 may be playing a key role in driving metaplastic inflammation and early disease. In contrast, stromal expression levels of caspase-1 increased with disease progression with the highest values in 9- and 12-month-old mice (Fig. 3c). This result correlated with histological values for inflammation and neoplastic progression at the SCJ in L2-IL-1B mice ($p < 0.05$) (Fig. 3e, f), suggesting that caspase-1 expressed within inflammatory infiltrates of BE metaplasia regions may contribute to inflammation-associated disease progression.

Metaplastic regions of EAC patient resection tissue display elevated epithelial caspase-1 expression levels.

We next sought to determine whether similar caspase-1 expression patterns occurred during disease progression in EAC patients. TMAs were generated from areas of patient-matched adjacent normal tissue, BE metaplasia and EAC within esophageal resection tissue from 32 patients (Table 1). The TMAs were stained and scored for caspase-1 expression levels.

Similar to previous observations from the murine and in vitro models, we observed significantly higher levels of epithelial caspase-1 expression in metaplastic tissue ($p < 0.01$) compared to normal esophageal tissue, but not in tumor tissue (Fig. 4a, b). *CASP1* gene expression was also higher in BE tissue when compared to matched normal gastric cardia (Supplementary fig. 1). As expected, stromal caspase-1 expression scores were higher in metaplastic and tumor regions, when compared to less inflamed adjacent normal tissue, although differences were not statistically significant (Fig. 4a, c).

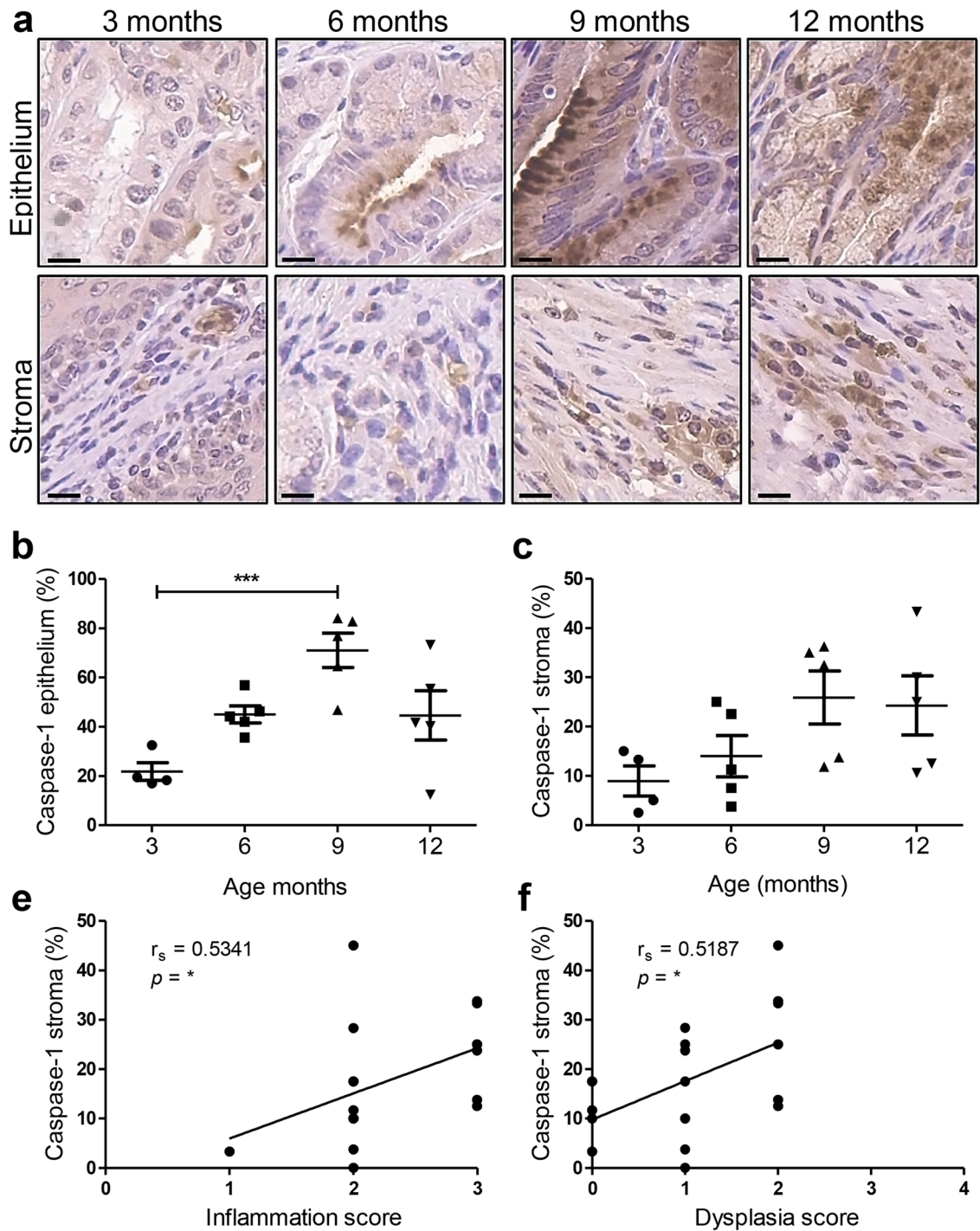


Fig. 3 Epithelial caspase-1 expression is upregulated during BE metaplasia in L2-IL-1B mice. **a** Representative images of caspase-1 IHC staining in BE regions at the SCJ in L2-IL-1B mice at 3 ($n=4$), 6 ($n=5$), 9 ($n=5$) and 12 ($n=5$) months. Images taken at $20\times$ magnification, scale bars = $10\ \mu\text{m}$. Graphs represent cytoplas-

mic caspase-1 positivity (%) of **b** columnar epithelium and **c** stroma within the BE region. Data represent mean \pm SEM. One-way ANOVA followed by Tukey's post hoc test. Correlation of stromal caspase-1 expression (%) versus scores for **d** inflammation and **e** dysplasia. r_s = Spearman's correlation coefficient, $*p < 0.05$, $***p < 0.001$

Table 1 EAC Patient characteristics

Patient no	NAT	Differentiation	Grade	Lymph node
1	No	Poor	Not stated	2/8 positive
2	Yes	Moderate	Not stated	Negative
3	No	Moderate	Not stated	19 negative
4	No	Poor	Not stated	11 negative
5	Yes	Moderate	ypT2N0Mx	Negative
7	No	Moderate	Not stated	5/17 positive
9	Yes	Poor	yPT3N1Mx	1 positive
10	No	Well	pT1N0Mx	Negative
11	Yes	Poor	ypT3, N1	3/10 positive
12	No	Moderate	pT3N1Mx	4/6 positive
14	No	Moderate	Not stated	7 negative
15	No	Moderate to poor	T1cN0Mx	25 negative
16	No	Moderate	pT3N1Mx	4/14 positive
17	No	Poor	pT3N1Mx	4/10 positive
18	No	–	pT1N0Mx	22 negative
19	Yes	Poor	ypT3N1Mx	1/10 positive
20	Yes	Moderate	yPT2N0Mx	40 negative
21	No	Poor	pT3N0(ITC)Mx	19 negative
22	Yes	–	ypT2N0Mx	5 negative
23	No	Well	pT3N0Mx	10 positive
24	No	Moderate-poor	pT3pN1Mx	5/12 positive
25	No	Poor	pT2N0Mx	14 negative
27	Yes	Moderate	yPT3N1	1/8 negative
28	No	Moderate	ypT3N0Mx	12 negative
29	Yes	Moderate	ypT1N1Mx	2/7 positive
30	Yes	Poor	pT3N1Mx	2/17 positive
31	Yes	Moderate	ypT3N1Mx	3/18 positive
32	Yes	Moderate-poor	pT3N2Mx	6/17 positive
34	Yes	Poor	ypT3N1Mx	1/9 positive
35	No	Moderate-well	pT1	Negative
38	No	Moderate	pT1bN0Mx	Negative
39	No	Moderate	pT1aN0Mx	17 negative

Biopsies from BE regions secrete higher levels of inflammatory mediators, compared to adjacent normal biopsies

Ex vivo explant culture of BE patient biopsy tissue (metaplastic and matched normal) was subsequently carried out to characterize the inflammatory cytokine secretion profile of metaplastic BE tissue, particularly regarding IL-1 β and IL-18, as their secretion is directly dependent on caspase-1. Explant biopsies were taken from previously diagnosed BE patients ($n = 10$) undergoing routine surveillance endoscopies. Patient characteristics are shown in Table 2. For each patient, biopsies were taken from the identified areas of metaplasia ($\times 2$) and normal squamous epithelium ($\times 2$). Analysis of culture supernatants confirmed that BE explant tissues demonstrated higher levels

of IL-1 β , IL-6, IL-8 and IFN- γ ($p < 0.01$), when compared to adjacent normal tissue (Fig. 5a, c–e). Elevated levels of these inflammatory cytokines have been reported by other studies [10, 15, 24]. In contrast, levels of IL-18 secretion were reduced ($p < 0.01$) in BE explants compared to adjacent normal tissue (Fig. 5b). Analysis of pro-*IL1B* and pro-*IL18* mRNA expression in two publicly available BE patient datasets [25, 26] showed that pro-*IL1B* mRNA is significantly increased, while pro-*IL18* mRNA levels are significantly lower in BE tissue, compared to adjacent normal tissue (Supplementary fig. 2a–d). These observations suggest that the columnar epithelial cells of metaplastic tissue have a lower constitutive pro-IL-18 expression compared to adjacent normal squamous tissue.

Effect of caspase-1 inhibition on inflammatory cytokine secretion in BE patient biopsies

To determine the functional role of caspase-1, normal and BE explants ($n = 10$ patients) were cultured in the presence or absence of a tetra-peptide caspase-1 inhibitor (WEHD.CHO). A dose response analysis of WEHD.CHO carried out in activated THP-1 macrophages revealed that caspase-1 activity was optimally inhibited at 10 μ M, as indicated by reduced levels of IL-1 β secretion (Fig. 6a). Analysis of supernatants from the biopsy cultures revealed no significant differences in LDH secretion between WEHD.CHO-treated and -untreated groups, indicating no cytotoxic effect of WEHD.CHO (Fig. 6b). Analysis of inflammatory cytokines from the supernatants revealed varying levels of caspase-1 inhibitor efficacy (Fig. 6c–f). 50% of patients showed reduced IL-1 β secretion, and 60% of patients showed reduced IL-8 secretion, in response to inhibitor treatment (Fig. 6c, f). These results highlight the inter-patient variability and heterogeneity associated with patient biopsy analysis.

Further separation of cytokine secretion profiles based on patient obesity status (BMI, obese ≥ 30 kg/m²) revealed that obese BE patients had slightly higher, although not significant, IL-1 β and IL-18 secretion levels (Supplementary fig. 3a, b). In response to caspase-1 inhibition, 4/6 obese BE patients had reduced IL-1 β secretion with no obvious differences observed for IL-18 secretion (Supplementary fig. 3c, d). These results suggest that caspase-1 inhibition may limit inflammation in BE patients, particularly those with obesity. However, inhibitor analysis in a larger BE patient cohort is required for this to be statistically confirmed.

Caspase-1 inhibition limits the secretion of IL-1 β and CXCL1 in BE organoid cultures

To further explore the importance of caspase-1 activity during metaplasia, BE organoids from 12-month-old L2-IL-1B mice were cultured and stimulated with LPS in the presence

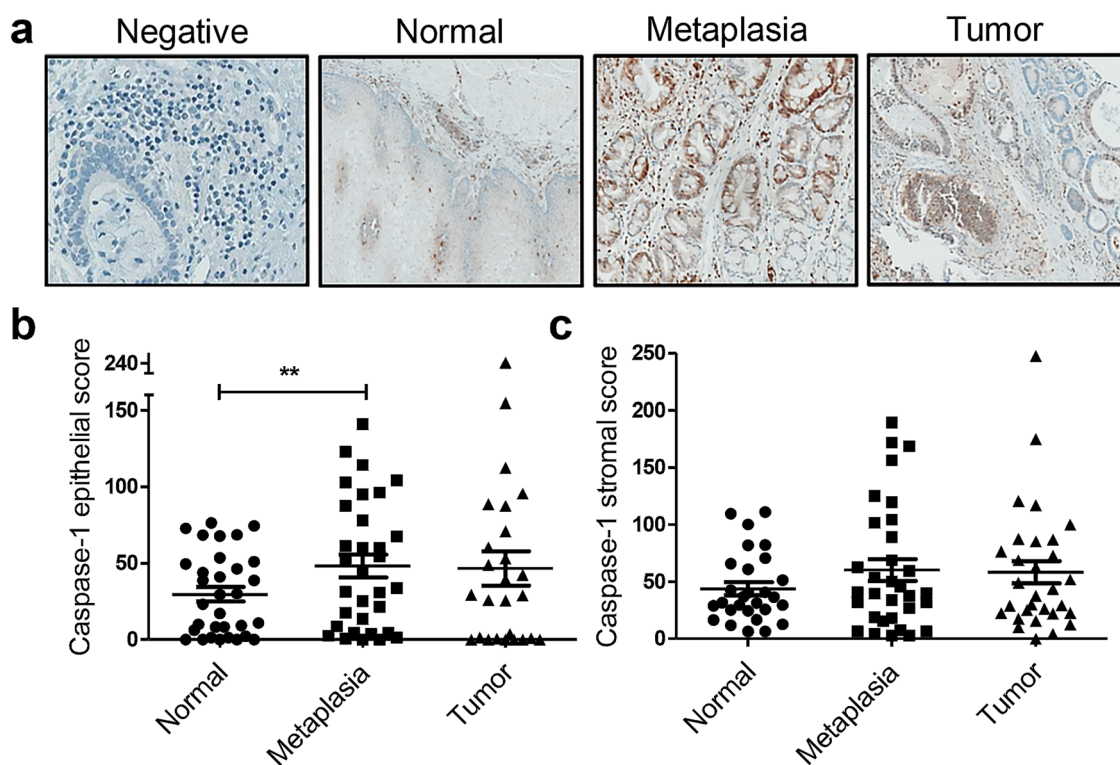


Fig. 4 Metaplastic regions of EAC patient resection tissue display elevated epithelial caspase-1 expression levels. **a** Representative images of caspase-1 IHC staining in epithelial and stromal cells in histologically defined areas of normal, metaplasia and tumor. Magnification 20 × (Leica Biosystems). Caspase-1 IHC scores in **b** epi-

thelium (normal, metaplasia and tumor ($n=32, 32, 26$, respectively)) and **c** stroma (normal, metaplasia and tumor ($n=28, 32, 30$, respectively)). Data represent mean \pm SEM. Wilcoxon signed-rank test: ** $p < 0.01$

Table 2 Barrett's esophagus patient characteristics

Patient	Age	Sex	Weight (kg)	BMI (kg/m ²)	Prague classification	Vienna grade
1	51	M	111.6	36.03	C0M3	1
2	77	F	89.2	40.72	C1M3	1
3	69	M	74.4	24.43	C12M12	3
4	64	F	89.6	37.78	C5M9	1
5	62	M	82	26.78	C0M5	1
6	77	F	56.3	24.69	C2M3	1
7	57	M	94	28.69	C1M2	1
8	86	M	81.9	28.01	C1M5	1
9	59	M	96.2	33.29	C1M2	4
10	49	M	109	37.64	C0M6	1

or absence of WEHD.CHO (Fig. 7). Representative images of untreated metaplastic organoids are shown at 0, 24 and 48 h (Fig. 7a). Although organoid growth plots revealed no significant differences in proliferation between groups (Fig. 7b), we observed reduced IL-1 β ($p < 0.01$) secretion in the presence of the caspase-1 inhibitor in LPS-stimulated organoids (Fig. 7d). BE organoids secreted low levels of IL-6, with no significant

differences observed between treatment groups (Fig. 7e). In contrast, significant secretion of the murine IL-8 orthologs CXCL1 and CXCL2 ($p < 0.01$) occurred in response to LPS stimulation (Fig. 7f, g). In the presence of the caspase-1 inhibitor, reductions in CXCL2 secretion were not found to be significant; however CXCL1 secretion from stimulated organoids was significantly reduced ($p < 0.05$) (Fig. 7f, g).

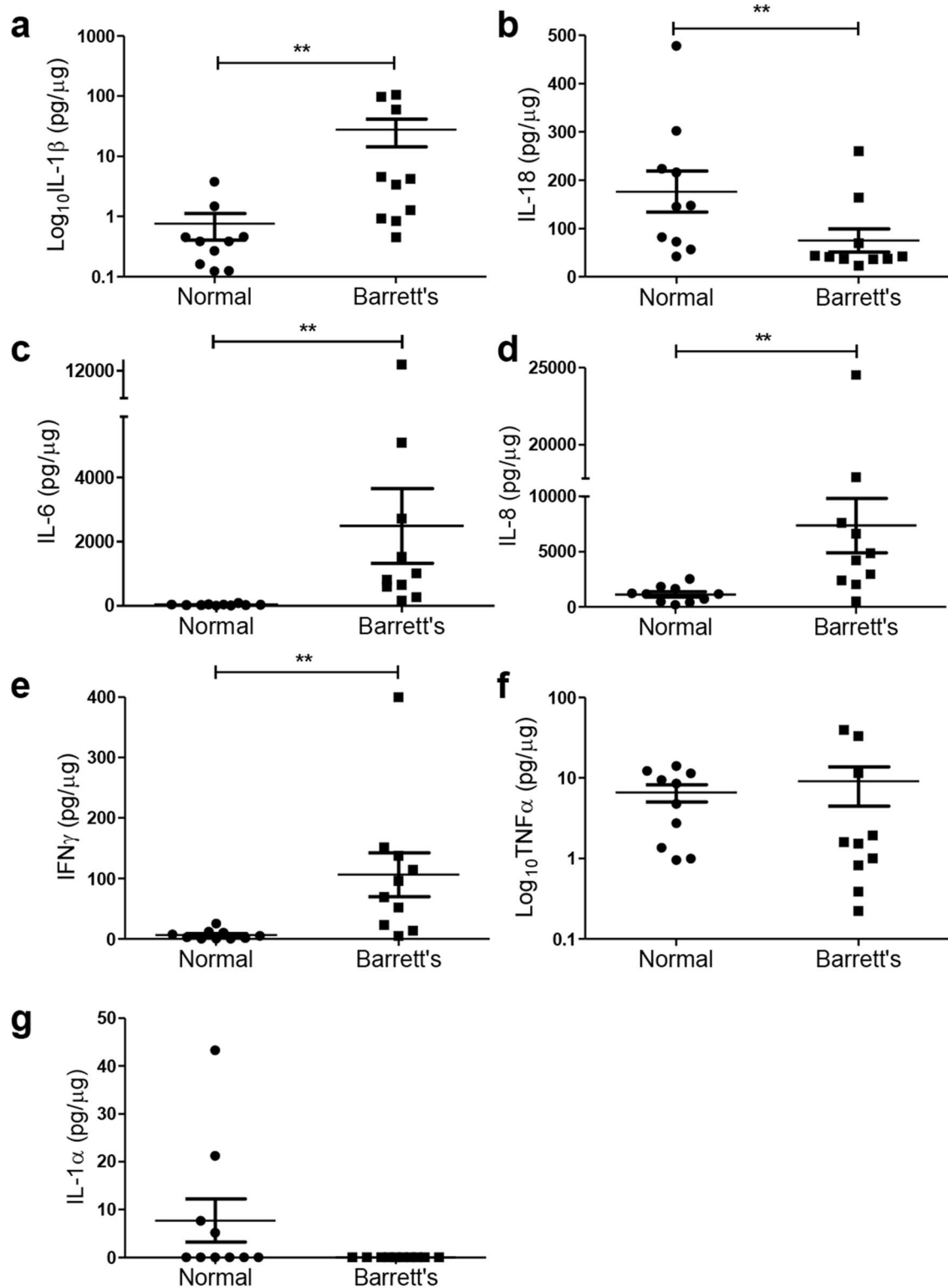


Fig. 5 Biopsies from BE regions secrete higher levels of inflammatory mediators, compared to adjacent normal biopsies. Matched esophageal biopsies were taken from diagnosed BE patients ($n=10$) from BE and adjacent normal regions. Explant biopsies were cultured for 16 h and culture supernatants were subsequently measured for

levels of inflammatory mediators and normalized to total protein: **a** IL-1 β , **b** IL-18, **c** IL-6, **d** IL-8, **e** IFN- γ , **f** TNF α and **g** IL-1 α (pg/ μg). Cytokines were measured using MSD multiplex analysis (**a–c**) and ELISA (**d–g**). Data represents mean \pm SEM. Wilcoxon signed-rank test: ** $p < 0.01$

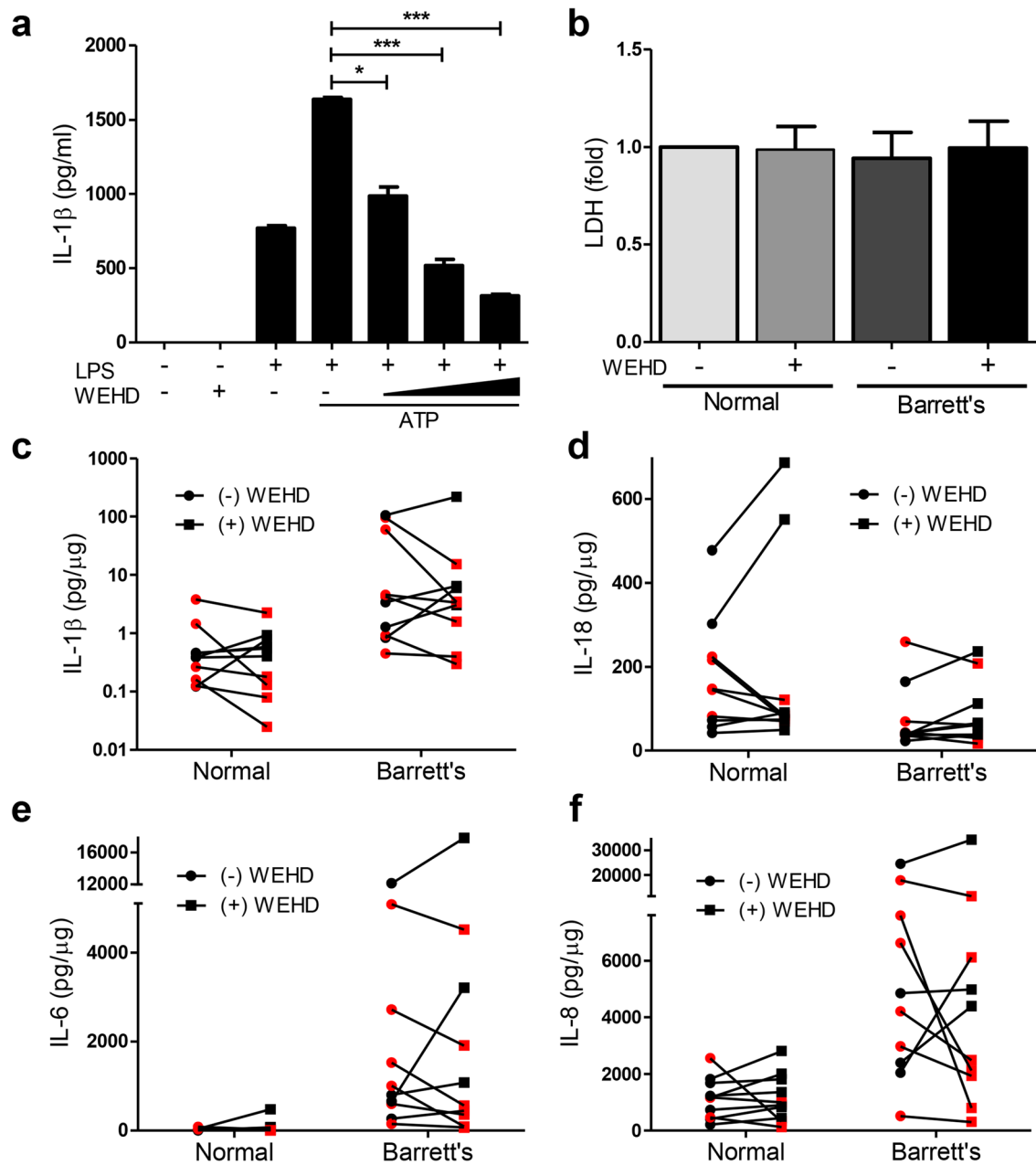


Fig. 6 Effect of caspase-1 inhibition on inflammatory cytokine secretion in BE patient biopsies. **a** Dose response of caspase-1 inhibitor, WEHD.CHO (Trp-Glu-His-Asp-aldehyde) (1 μ M, 5 μ M, 10 μ M) in the THP-1 cell line. Cells were PMA stimulated (10 ng/mL, 48 h) prior to LPS stimulation (1 μ g/mL, 18 h), followed by ATP stimulation (5 mM, 30 min). Graph is representative of three independent experiments. Paired Student's *t* test: * p < 0.05, *** p < 0.001. **b-f** Matched esophageal biopsy explants were taken from areas of BE

and adjacent normal tissue from previously diagnosed BE patients ($n = 10$). Esophageal explants were cultured with or without WEHD.CHO (10 μ M) for 16 h. **b** Cytotoxicity assay measuring LDH levels in supernatants from adjacent normal and BE explants. Data represents mean \pm SEM. Secretion of inflammatory mediators **c** IL-1 β , **d** IL-18, **e** IL-6 and **f** IL-8 (pg/ μ g) were measured using MSD multiplex analysis (**c**, **d**) and ELISA (**e**, **f**). Two-way ANOVA followed by Bonferroni's post-test: non-significant

Discussion

This study characterizes the expression of caspase-1 during esophageal disease, confirming that stromal caspase-1 expression correlates with histological inflammation during

disease progression (Normal-BE-EAC). A selective over-expression pattern for epithelial caspase-1 during BE metaplasia was identified, and caspase-1 inhibitor experiments suggest that caspase-1 mediates the production of disease-associated inflammatory factors during esophageal disease

progression. We and others have observed that inflammation is a main driver of disease progression in BE and therefore anti-inflammatory strategies directed against the inflammatory might emerge as preventative therapies [1, 5].

Although the majority of inflammasome studies have been performed in innate immune cells, active inflammasome complexes have been identified in epithelial cells derived from mucosa including the skin, intestine and lung [27]. A study by Nadatani et al. supports our findings, showing that NLRP3 inflammasome activation occurs in LPS-stimulated BE cell lines, but not in normal squamous cells, resulting in IL-1 β secretion [15]. A rationale for this observation may be provided by our data, which employed three separate model systems to confirm that caspase-1 expression is significantly higher in BE, compared to normal squamous epithelial cells. Our data suggests that increased availability of caspase-1, which associates with ASC and upregulated NLRP3 following LPS priming, contributes to the increased NLRP3 activity observed in BE epithelial cells.

There are many examples of inflammasome signaling driving inflammation-associated carcinogenesis, identifying caspase-1 as a common instigator and driver of disease [28, 29]. However, inflammasomes are also attributed with roles in anti-tumor immunity during carcinogenesis [30]. In our study, caspase-1 expression was undetectable in the two EAC cell lines used in the cell line disease progression model, while in the murine model epithelial caspase-1 expression levels appeared to decrease once a more dysplastic phenotype had developed. Similar observations have been made in inflamed and tumorigenic colon tissue, where a trend toward elevated epithelial caspase-1 expression in inflamed tissue, but lower levels in tumor tissue from colitis-associated colorectal cancer (CRC) patients was shown [31]. In the context of non-GI adenocarcinomas, caspase-1 expression is also significantly lower in tumor compared to adjacent tissue in both breast and prostate [32, 33]. These observations suggest that tumor-induced suppression of caspase-1 expression, and thus inflammasome activity, may be occurring in established EAC cells, highlighting the complexity of inflammasome signaling during cancer progression.

BE is a mosaic of metaplastic subtypes, displaying significant heterogeneity on a cellular and molecular level. Inflammation is maximal at the SCJ and is characterized by increased levels of IL-1 β and IL-8, the expression of

which is stimulated by the interaction between immune cells and epithelia at the SCJ [10]. As part of its pro-inflammatory effect, IL-1 β induces the expression of IL-8/CXCL1 chemokines [34, 35]. Consistent with metaplastic heterogeneity, data generated from BE patient biopsies were variable in terms of caspase-1 inhibition effects, with observed reduction in IL-1 β and IL-8 secretion in 50% and 60% of patients, respectively. However, a trend toward a greater IL-1 β reduction in inhibitor-treated obese patient explants, compared to those from non-obese patients was observed. This is an interesting observation, as both BE and EAC risks are strongly related to obesity and weight gain [36, 37]. Additionally, the Irish National Barrett's Registry has previously reported that approximately 76% of Barrett's patients are overweight or obese [38].

In the transgenic BE mouse model (L2-IL-1B), epithelial CXCL1 and IL-8 have recently been implicated in neutrophil recruitment and accelerated disease progression during a high fat diet [5]. Results from this study show that LPS-stimulated BE organoids produce significant levels of the IL-8 orthologs, CXCL1 and CXCL2, supporting the hypothesis that metaplastic tissue responds to esophageal microbial stimuli in an inflammatory manner, as has recently been suggested [15]. Furthermore, incubation of LPS-stimulated BE organoids in the presence of a caspase-1 inhibitor resulted in significantly reduced IL-1 β and CXCL1 secretion, supporting a role for caspase-1 in BE pathogenesis.

In summary, we identify an association between caspase-1 signaling and metaplastic inflammation, which calls into question the therapeutic potential of targeting inflammasome pathways or caspase-1 activity in BE patients. Blocking IL-1 signaling, via anakinra, rilonacept or canakinumab, has been FDA approved to treat a broad spectrum of diseases, including rheumatoid arthritis, Crohn's disease and type II diabetes [39]. The CANTOS trial revealed significant reductions in lung cancer incidence and cancer mortality in a canakinumab-treated cohort of patients [40]. Similar to BE and associated EAC, lung cancer is epithelial derived and highly associated with chronic inflammation [2, 41]. It is therefore tempting to speculate that the mechanisms identified in this study could effectively be targeted by these drugs to help limit inflammation-induced acceleration of disease progression in BE patients. However, caution must also be taken, as data also suggests that caspase-1 is actively suppressed within established EAC tissue.

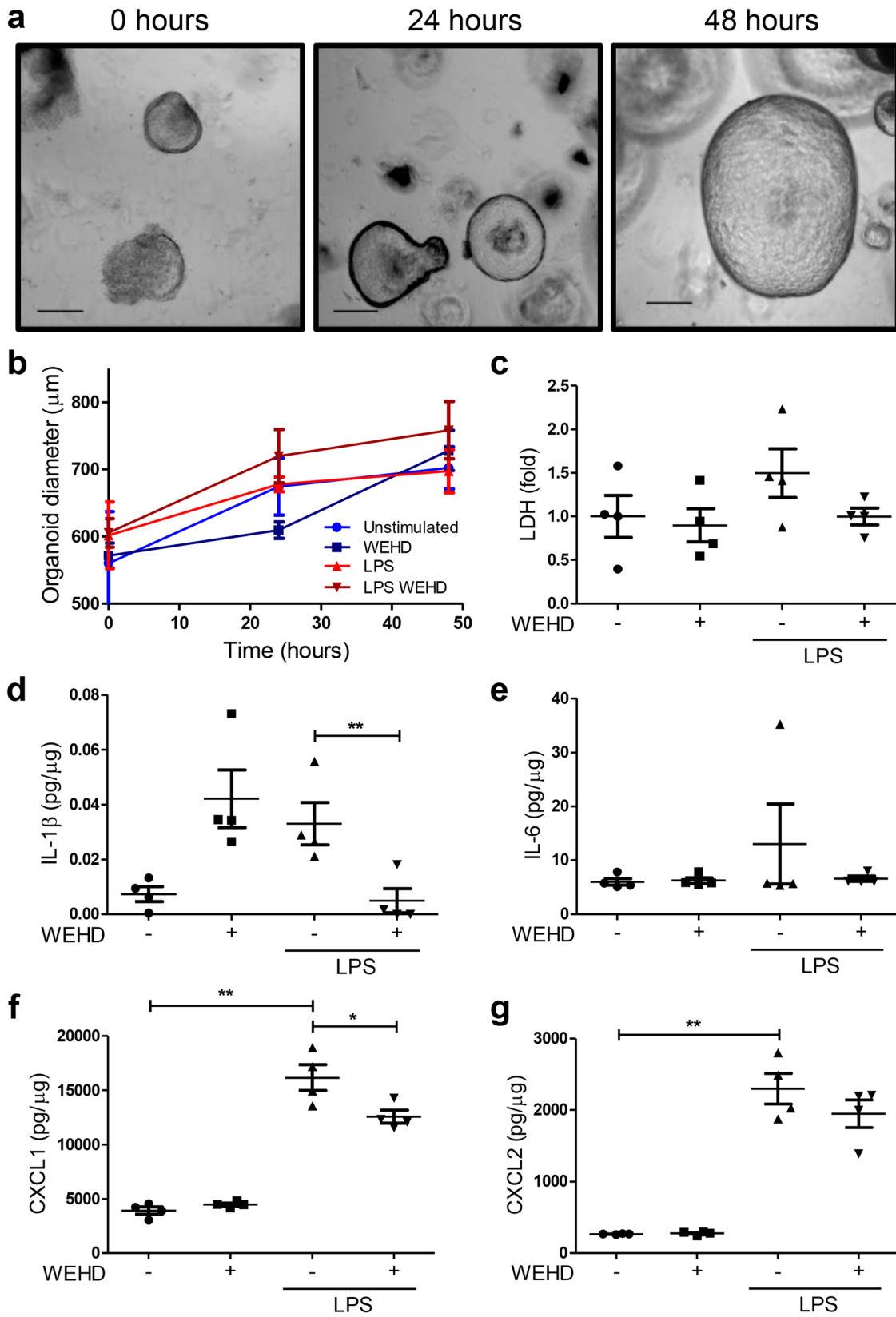


Fig. 7 Caspase-1 inhibition limits the secretion of IL-1 β and CXCL1 in BE organoid cultures. **a** Representative images of organoid cultures taken at 0, 24 and 48 h. Magnification: 5 \times . Scale bars: 200 μ m. **b** Growth curves ($n=3$) following treatments at 0, 24 and 48 h. Data is represented as \pm SEM. Organoid secretion levels ($n=4$) were analyzed for **c** LDH **d** IL-1 β , **e** IL-6, **f** CXCL1 and **g** CXCL2. Data was normalized to total organoid protein (pg/ μ g). Paired Student's *t* test: * $p < 0.05$, ** $p < 0.01$

Acknowledgements We would like to thank members of the gastroenterological and surgical teams in St. James's Hospital and Beaumont Hospital and all patients who gave their consent to partake in this study. The authors thank Glen Byrne for his help with digital images. This research was supported by a Trinity College 'John Scott Fellowship' and an EU Horizon 2020 Marie Skłodowska-Curie ITN 'TRACT', grant agreement No 721906.

Author contributions GB, JOS and EMC are responsible for study conceptualization. GB generated most of the data, assisted by AA, JK and MQ for mice studies; and KO, JP, AH, EF, NC, JW, BF, HON and EK for human studies. DT, FMC, NR and JR contributed clinical specimens. JOS provided resources, supervision and editing. EMC provided funding and supervision. GB and EMC wrote and edited the manuscript. GB is the guarantor of this work and, as such, had full access to all the data in the study and takes responsibility for the integrity of the data and the accuracy of the data analysis.

Funding G.B. is supported by a Trinity College 'John Scott Fellowship'. E.F. is an Early Stage Researcher of the EU Horizon 2020 Research and Innovation Programme (Marie Skłodowska-Curie grant agreement No 721906). M.Q. is supported by Deutsche Krebshilfe Max Eder Program.

Data availability The datasets analyzed during the current study are available in the GEO DataSets repository, NCBI, GSE34619, GSE1420.

Compliance with ethical standards

Conflict of interest The authors have no conflicts of interest to declare.

Ethical approval and ethical standards All research was conducted in accordance with the ethical standards of the institution and country in which the research took place. Murine studies were performed at Technische Universität München (TUM), Germany, in accordance with German Animal Welfare and Ethical Guidelines and approved by the District Government of Bavaria. Ethical approval for patient research was granted by the St. James's Hospital/AMNCH Review Board and Beaumont Hospital Ethics committee. This was concurrent with the 1964 Helsinki Declaration and later amendments.

Informed consent Informed written patient consent was obtained for the use of patient tissue and data prior to inclusion in this study. Publication of this data has additionally been consented. Patient data were pseudo-anonymized prior to sample access.


References

1. Quante M, Graham TA, Jansen M (2018) Insights into the pathophysiology of esophageal adenocarcinoma. *Gastroenterology* 154:406–420
2. Picardo SL, Maher SG, O'Sullivan JN, Reynolds JV (2012) Barrett's to oesophageal cancer sequence: a model of inflammatory-driven upper gastrointestinal cancer. *Dig Surg* 29:251–260
3. Spechler SJ, Souza RF (2014) Barrett's esophagus. *N Engl J Med* 371:836–845
4. Hvid-Jensen F, Pedersen L, Drewes AM, Sorensen HT, Funch-Jensen P (2011) Incidence of adenocarcinoma among patients with Barrett's esophagus. *N Engl J Med* 365:1375–1383
5. Munch NS, Fang HY, Ingermann J, Maurer HC, Anand A, Kellner V, Sahn V, Wiethaler M, Baumeister T, Wein F, Einwächter H, Bolze F, Klingenspor M, Haller D, Kavanagh M, Lysaght J, Friedman R, Dannenberg AJ, Pollak M, Holt PR, Muthupalani S, Fox JG, Whary MT, Lee Y, Ren TY, Elliot R, Fitzgerald R, Steiger K, Schmid RM, Wang TC, Quante M (2019) High-fat diet accelerates carcinogenesis in a mouse model of Barrett's esophagus via interleukin 8 and alterations to the gut microbiome. *Gastroenterology* 157:492–506.e492
6. Creagh EM (2014) Caspase crosstalk: integration of apoptotic and innate immune signalling pathways. *Trends Immunol* 35:631–640
7. Mariathasan S, Weiss DS, Newton K, McBride J, O'Rourke K, Roose-Girma M, Lee WP, Weinrauch Y, Monack DM, Dixit VM (2006) Cryopyrin activates the inflammasome in response to toxins and ATP. *Nature* 440:228–232
8. Shi J, Zhao Y, Wang K, Shi X, Wang Y, Huang H, Zhuang Y, Cai T, Wang F, Shao F (2015) Cleavage of GSDMD by inflammatory caspases determines pyroptotic cell death. *Nature* 526:660–665
9. Karan D (2018) Inflammasomes: emerging central players in cancer immunology and immunotherapy. *Front Immunol* 9:3028–3028
10. Fitzgerald RC, Abdalla S, Onwuegbusi BA, Sirieix P, Saeed IT, Burnham WR, Farthing MJ (2002) Inflammatory gradient in Barrett's oesophagus: implications for disease complications. *Gut* 51:316–322
11. Shrivastava MS, Hussain Z, Giricz O, Shenoy N, Polineni R, Maitra A, Verma A (2014) Targeting chemokine pathways in esophageal adenocarcinoma. *Cell Cycle* 13:3320–3327
12. Campos VJ, Mazzini GS, Juchem JF, Gurski RR (2020) Neutrophil-lymphocyte ratio as a marker of progression from non-dysplastic Barrett's esophagus to esophageal adenocarcinoma: a cross-sectional retrospective study. *J Gastrointest Surg* 24:8–18
13. Quante M, Bhagat G, Abrams JA, Marache F, Good P, Lee MD, Lee Y, Friedman R, Asfaha S, Dubeykovskaya Z, Mahmood U, Figueiredo JL, Kitajewski J, Shawber C, Lightdale CJ, Rustgi AK, Wang TC (2012) Bile acid and inflammation activate gastric cardia stem cells in a mouse model of Barrett-like metaplasia. *Cancer Cell* 21:36–51
14. Ponten F, Jirstrom K, Uhlen M (2008) The human protein atlas—a tool for pathology. *J Pathol* 216:387–393
15. Nadatani Y, Huo X, Zhang X, Yu C, Cheng E, Zhang Q, Dunbar KB, Theiss A, Pham TH, Wang DH, Watanabe T, Fujiwara Y, Arakawa T, Spechler SJ, Souza RF (2016) NOD-like receptor protein 3 inflammasome priming and activation in Barrett's epithelial cells. *Cell Mol Gastroenterol Hepatol* 2:439–453
16. Nakagawa H, Wang TC, Zukerberg L, Odze R, Togawa K, May GHW, Wilson J, Rustgi AK (1997) The targeting of the cyclin D1 oncogene by an Epstein-Barr virus promoter in transgenic mice causes dysplasia in the tongue, esophagus and forestomach. *Oncogene* 14:1185

17. Fox JG, Beck P, Dangler CA, Whary MT, Wang TC, Shi HN, Nagler-Anderson C (2000) Concurrent enteric helminth infection modulates inflammation and gastric immune responses and reduces helicobacter-induced gastric atrophy. *Nat Med* 6:536–542
18. Schellnegger R, Quante A, Rospleszcz S, Schernhammer M, Höhl B, Tobiasch M, Pastula A, Brandtner A, Abrams JA, Strauch K, Schmid RM, Vieth M, Wang TC, Quante M (2017) Goblet-cell ratio in combination with differentiation and stem cell markers in Barrett's esophagus allow distinction of patients with and without esophageal adenocarcinoma. *Cancer Prevent Res (Philadelphia, Pa)* 10:55–66
19. Pastula A, Middelhoff M, Brandtner A, Tobiasch M, Hohl B, Nuber AH, Demir IE, Neupert S, Kollmann P, Mazzuoli-Weber G, Quante M (2016) Three-dimensional gastrointestinal organoid culture in combination with nerves or fibroblasts: a method to characterize the gastrointestinal stem cell niche. *Stem Cells Int* 2016:3710836
20. Phelan JJ, MacCarthy F, Feighery R, O'Farrell NJ, Lynam-Lennon N, Doyle B, O'Toole D, Ravi N, Reynolds JV, O'Sullivan J (2014) Differential expression of mitochondrial energy metabolism profiles across the metaplasia-dysplasia-adenocarcinoma disease sequence in Barrett's oesophagus. *Cancer Lett* 354:122–131
21. Rano TA, Timkey T, Peterson EP, Rotonda J, Nicholson DW, Becker JW, Chapman KT, Thornberry NA (1997) A combinatorial approach for determining protease specificities: application to interleukin-1 β converting enzyme (ICE). *Chem Biol* 4:149–155
22. Benkova B, Lozanov V, Ivanov IP, Mitev V (2009) Evaluation of recombinant caspase specificity by competitive substrates. *Anal Biochem* 394:68–74
23. Rozman-Pungercar J, Kopitar-Jerala N, Bogyo M, Turk D, Vasiljeva O, Stefe I, Vandenabeele P, Bromme D, Puizdar V, Fonovic M, Trstenjak-Prebanda M, Dolenc I, Turk V, Turk B (2003) Inhibition of papain-like cysteine proteases and legumain by caspase-specific inhibitors: when reaction mechanism is more important than specificity. *Cell Death Differ* 10:881–888
24. Kavanagh ME, Conroy MJ, Clarke NE, Gilmartin NT, O'Sullivan KE, Feighery R, MacCarthy F, O'Toole D, Ravi N, Reynolds JV, O'Sullivan J, Lysaght J (2016) Impact of the inflammatory microenvironment on T-cell phenotype in the progression from reflux oesophagitis to Barrett oesophagus and oesophageal adenocarcinoma. *Cancer Lett* 370:117–124
25. di Pietro M, Lao-Sirieix P, Boyle S, Cassidy A, Castillo D, Saadi A, Eskeland R, Fitzgerald RC (2012) Evidence for a functional role of epigenetically regulated midcluster HOXB genes in the development of Barrett esophagus. *Proc Natl Acad Sci USA* 109:9077–9082
26. Kimchi ET, Posner MC, Park JO, Darga TE, Kocherginsky M, Karrison T, Hart J, Smith KD, Mezhir JJ, Weichselbaum RR, Khodarev NN (2005) Progression of Barrett's metaplasia to adenocarcinoma is associated with the suppression of the transcriptional programs of epidermal differentiation. *Cancer Res* 65:3146–3154
27. Santana PT, Martel J, Lai H-C, Perfettini J-L, Kanellopoulos JM, Young JD, Coutinho-Silva R, Ojcius DM (2016) Is the inflammasome relevant for epithelial cell function? *Microbes Infect* 18:93–101
28. Kopalli SR, Kang TB, Lee KH, Koppula S (2018) NLRP3 Inflammasome activation inhibitors in inflammation-associated cancer immunotherapy: an update on the recent patents. *Recent Pat Anti-cancer Drug Discov* 13:106–117
29. Guo B, Fu S, Zhang J, Liu B, Li Z (2016) Targeting inflammasome/IL-1 pathways for cancer immunotherapy. *Sci Rep* 6:36107
30. Ghiringhelli F, Apetoh L, Tesniere A, Aymeric L, Ma Y, Ortiz C, Vermaelen K, Panaretakis T, Mignot G, Ullrich E, Perfettini JL, Schlemmer F, Tasdemir E, Uhl M, Genin P, Civas A, Ryffel B, Kanellopoulos J, Tschopp J, Andre F, Lidereau R, McLaughlin NM, Haynes NM, Smyth MJ, Kroemer G, Zitvogel L (2009) Activation of the NLRP3 inflammasome in dendritic cells induces IL-1 β -dependent adaptive immunity against tumors. *Nat Med* 15:1170–1178
31. Flood B, Oficjalska K, Laukens D, Fay J, O'Grady A, Caiazza F, Heetun Z, Mills KH, Sheahan K, Ryan EJ, Doherty GA, Kay E, Creagh EM (2015) Altered expression of caspases-4 and -5 during inflammatory bowel disease and colorectal cancer: diagnostic and therapeutic potential. *Clin Exp Immunol* 181:39–50
32. Sun Y, Guo Y (2018) Expression of caspase-1 in breast cancer tissues and its effects on cell proliferation, apoptosis and invasion. *Oncol Lett* 15:6431–6435
33. Winter RN, Kramer A, Borkowski A, Kyprianou N (2001) Loss of caspase-1 and caspase-3 protein expression in human prostate cancer. *Cancer Res* 61:1227–1232
34. Biondo C, Mancuso G, Midiri A, Signorino G, Domina M, Lanza Cariccio V, Mohammadi N, Venza M, Venza I, Teti G, Beninati C (2014) The interleukin-1 β /CXCL1/2/neutrophil axis mediates host protection against group B streptococcal infection. *Infect Immun* 82:4508–4517
35. Lee C-H, Syu S-H, Liu K-J, Chu P-Y, Yang W-C, Lin P, Shieh W-Y (2015) Interleukin-1 beta transactivates epidermal growth factor receptor via the CXCL1-CXCR2 axis in oral cancer. *Oncotarget* 6:38866–38880
36. Kubo A, Cook MB, Shaheen NJ, Vaughan TL, Whiteman DC, Murray L, Corley DA (2013) Sex-specific associations between body mass index, waist circumference and the risk of Barrett's oesophagus: a pooled analysis from the international BEACON consortium. *Gut* 62:1684–1691
37. Turati F, Tramacere I, La Vecchia C, Negri E (2013) A meta-analysis of body mass index and esophageal and gastric cardia adenocarcinoma. *Ann Oncol* 24:609–617
38. Picardo SL, O'Brien MP, Feighery R, O'Toole D, Ravi N, O'Farrell NJ, O'Sullivan JN, Reynolds JV (2015) A Barrett's esophagus registry of over 1000 patients from a specialist center highlights greater risk of progression than population-based registries and high risk of low grade dysplasia. *Dis Esophagus* 28:121–126
39. Dinarello CA, Simon A, van der Meer JWM (2012) Treating inflammation by blocking interleukin-1 in a broad spectrum of diseases. *Nat Rev Drug Discovery* 11:633–652
40. Ridker PM, Everett BM, Thuren T, MacFadyen JG, Chang WH, Ballantyne C, Fonseca F, Nicolau J, Koenig W, Anker SD, Kastelein JJP, Cornel JH, Pais P, Pella D, Genest J, Cifkova R, Lorenzatti A, Forster T, Kobalava Z, Vida-Simiti L, Flather M, Shimokawa H, Ogawa H, Dellborg M, Rossi PRF, Troquay RPT, Libby P, Glynn RJ (2017) Antiinflammatory therapy with canakinumab for atherosclerotic disease. *N Engl J Med* 377:1119–1131
41. Borthwick LA (2016) The IL-1 cytokine family and its role in inflammation and fibrosis in the lung. *Semin Immunopathol* 38:517–534

Publisher's Note Springer Nature remains neutral with regard to jurisdictional claims in published maps and institutional affiliations.

Affiliations

Gillian Barber^{1,2} · Akanksha Anand³ · Katarzyna Oficjalska¹ · James J. Phelan² · Aisling B. Heeran² · Ewelina Flis¹ · Niamh E. Clarke² · Jenny A. Watson⁴ · Julia Strangmann³ · Brian Flood¹ · Hazel O'Neill² · Dermot O'Toole⁵ · Finbar MacCarthy⁵ · Narayanasamy Ravi^{2,5} · John V. Reynolds^{2,5} · Elaine W. Kay⁴ · Michael Quante³ · Jacintha O'Sullivan² · Emma M. Creagh¹ 

¹ School of Biochemistry and Immunology, Trinity Biomedical Sciences Institute, Trinity College Dublin, Dublin 2, Ireland

² Department of Surgery, Trinity Translational Medicine Institute, Trinity College and St. James's Hospital Dublin, Dublin 8, Ireland

³ Department of Internal Medicine, Technical University of Munich, Munich, Germany

⁴ Royal College of Surgeons in Ireland and Beaumont Hospital, Dublin 9, Ireland

⁵ National Oesophageal and Gastric Centre, St. James's Hospital, Dublin 8, Ireland